

Theoretical and Experimental Considerations of Thermal Humidity Characteristics

Seok-Weon Choi** Ju-Hyeong Cho*, Hee-Jun Seo* and Sang-Seol Lee**

Space Test Department, Korea Aerospace Research Institute
Yusung P.O.Box 113, Teajon, Korea 305-600

Abstract

Thermal humidity characteristics were considered theoretically and experimentally. A Simply well-fitted correlation of a saturated vapor pressure-temperature curve of water was introduced based on Antoine equation to make theoretical prediction of relative humidity according to temperature variation. Characteristics of dew point were also examined theoretically and its relation with temperature and humidity was evaluated. The exact mass of water vapor in a specified humidity and temperature condition was estimated to provide useful insight into the idea about how much amount of water corresponds to a specified humidity and temperature condition in a confined system. A simple but well-fitting model of dehumidification process was introduced to anticipate the trend of relative humidity level during GN₂(gaseous nitrogen) purge process in a humidity chamber. Well-suitedness of this model was also verified by comparison with experimental data. The overall appearance and specification of two thermal humidity chambers were introduced which were used to perform various thermal humidity tests in order to yield useful data necessary to support validity of theoretical models.

Key word : humidity, temperature, dew point, vapor pressure, dehumidification

Nomenclature

A, B, C	: Constants in Antoine equation (Eq. (1)) (A = 8.08, B = 1737.62, C = 234.20 for water vapor)
I	: Volumetric flow rate of GN ₂ at the inlet port of the chamber
k	: Characteristic purge constant of a humidity chamber
M_w	: Molecular weight of water (= 18.01)
P	: Vapor pressure(torr)
P_{data}	: Vapor pressure from experimental data
$P_{fitting}$: Vapor pressure from a fitting curve of Antoine equation
$P_s(T)$: Saturated vapor pressure(torr) at temperature T(°C)
P_w	: Partial pressure of water vapor(torr)
RH	: Relative humidity(%)
R_u	: Universal gas constant (= 8.314 J/mol · K)
scfm	: Standard cubic feet per minute
T	: Temperature(°C)

* Researcher

** Principial Researcher

E-mail : schoi@kari.re.kr, TEL : 042-860-2453, FAX : 042-860-2234

T_{dew}	: Dew point($^{\circ}\text{C}$)
V_{air}	: Volumetric amount of air in the chamber
V_{CH}	: Inner volume of the chamber
V_{G}	: Volumetric amount of gaseous nitrogen in the chamber
$V_{\text{G,out}}$: Volumetric amount of gaseous nitrogen being exhausted through an exit port of the chamber
ρ_w	: Density of water vapor(g/m^3)

Introduction

The component which is used in satellite should be tested under space environments before launch. To simulate orbit condition, space simulator such as thermal vacuum chamber is used. Thermal vacuum test using thermal vacuum chamber is the only way to simulate space environment in ground. But it cost a lot of money to perform thermal vacuum test.

In case of less vacuum sensitive component test, thermal cycling test are usually performed for low cost. In the thermal cycling test, water condensing is usually occurred during temperature increasing mode after several cycle. (Water condensing is not occurred during temperature decreasing)[1].

In the thermal cycling test for space component, it is not allowed to water condensing for component protection. So it is very important to prevent water condensing during thermal cycling test for space component. To prevent water condensing in thermal cycling chamber, GN2 purge is usually used in space component test. But it is still difficult to make a humidity control chamber using GN2 purge without understanding thermal humidity characteristics in GN2 purge cycling chamber.

It is very useful to obtain a saturated vapor pressure-temperature curve in considering thermal humidity characteristics theoretically. Antoine equation gives good correlation for a saturated vapor pressure-temperature curve of many substances except for water[2]. As for water, this paper proposed well-fitted correlation for the experimental data of a saturated vapor pressure-temperature curve of water using Antoine equation. The saturated vapor pressure-temperature curve leads not only to theoretical anticipation of dew point where vapor starts to condense into a liquid form but also to good prediction about how relative humidity varies according to temperature variation in a confined system with no net change of the amount of water. The ideal-gas equation of state was utilized to obtain the mass of water vapor indicating certain humidity level and temperature. This paper also introduces theoretical model of dehumidification process by GN2 purge to evaluate the trend of variation of relative humidity level as GN2 purge is under way in a humidity chamber. Well-suitedness of this model was also verified by comparison with experimental data. The thermal humidity chambers that are located at SITC(Satellite Integration and Test Center) in KARI(Korea Aerospace Research Institute) were utilized to provide relevant data and support validity of theoretical analysis of thermal humidity characteristics. These chambers have the capabilities to perform thermal-humidity cycle tests for a variety of specimens whose functional performance should be checked and verified under various thermal humid conditions. These thermal humidity chambers also have the capabilities to simulate as extremely low temperature as -150°C by dehumidifying the chamber interior first and then injecting LN2(Liquid Nitrogen) through several nozzles located at the rear side of the chamber interior. Such low temperature test is to perform functional verification and confirm reliabilities of special components including satellite components such as solar panels and antennae.

This paper is to give more thorough and quantitative understanding of humidity characteristics by focusing on theoretical analysis of thermal humidity characteristics including dew point and dehumidification process that are validated by various test data using thermal humidity chambers.

Theoretical Approach of Humidity Characteristics

Relative Humidity and Dew Point

Humidity level is usually expressed by the unit of %RH where RH stands for relative humidity that is a ratio of actual vapor pressure to the saturated vapor pressure of water at a certain temperature. Therefore, the higher the temperature is, the lower the relative humidity is for a confined system with a constant amount of water vapor because the saturated vapor pressure of water increases with increasing temperature as shown in Fig. 1(a) which indicates the experimental data of saturated vapor pressure of water in the temperature range of 0 to 100 °C quoted from Table 5.6 in Lange's handbook[2]. Antoine equation gives good correlation with experimental data in the relation of saturated vapor pressure and corresponding temperature for a variety of substances in the following form.

$$\log(P_s(T)) = A - \frac{B}{T+C} \quad (1)$$

Constants A, B, C in Eq. (1) are given for various substances except for water vapor in Lange's handbook[2]. In this paper, these constants are estimated so that the error from the experimental data should be minimized by replotting the saturated vapor pressure curve into a linear form as shown in Fig. 1(b). As a result, the optimal coefficients A = 8.08, B = 1737.62, C = 234.20 gives the minimum error as following.

$$|Error(\%)| = \left| \frac{P_{fitting}(T) - P_{data}}{P_{data}} \right| < 0.15(\%) \text{ for } 0 < T < 100 \text{ } ^\circ\text{C} \quad (2)$$

Eq. (1) can, on the other hand, be used to predict dew point (T_{dew}) or boiling point at a certain vapor pressure (P). The terms of "dew point" and "boiling point" may be used differently according to the direction in phase change between liquid and gas, but they have the same value at a fixed vapor pressure. For example, if we assume that there is a system in atmospheric pressure where the vaporized water occupies half of the ambient pressure ($P_w = 380$ torr) at 100 °C and this system starts to undergo cool-down process, then water vapor starts to condense into a liquid form at dew point of $T = 81.7$ °C. Meanwhile, if an ambient pressure reduced to 380 torr, for example, during flight, liquid water in a pot being heated starts to boil into vapor at $T = 81.7$ °C. In order to anticipate dew point at certain temperature and humid level, actual partial pressure of water vapor shall first be calculated as below by using Eq. (1).

$$P_w = P_s(T) \times RH/100 = 10^{(A - \frac{B}{T+C})} \times RH/100 \quad (3)$$

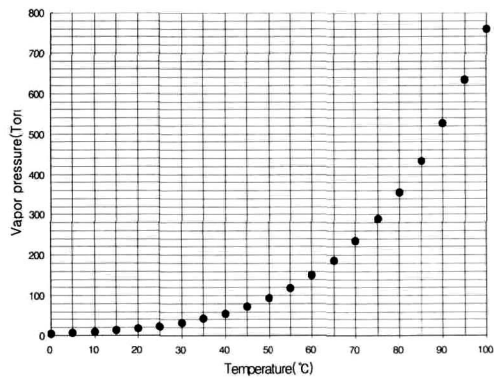
Now dew point can be obtained by combining Eqs. (1) and (3) as below.

$$\begin{aligned} T_{dew}(T, RH) &= \frac{B}{A - \log(P_w)} - C = \frac{B}{A - \log[10^{(A - \frac{B}{T+C})} \times RH/100]} - C \\ &= \frac{B}{\frac{B}{T+C} - \log(RH) + 2} - C \end{aligned} \quad (4)$$

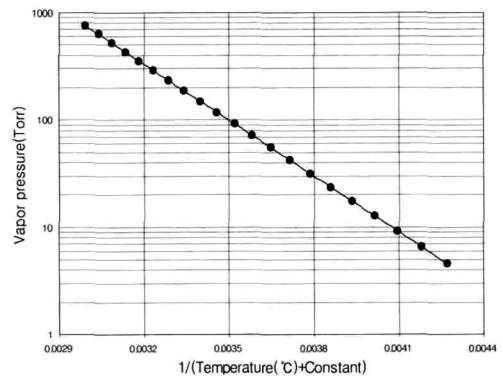
For example, in case of $T = 50$ °C with relative humidity of 40 %RH, dew point, $T_{dew}(50,40)$, is 32.6 °C using Eq. (4). For the purpose of comparison with experimental data, dew point can also be estimated from Table 5.6 in Lange's Handbook, in which the saturated vapor pressure at 50 °C is 92.51(torr), hence the actual vapor pressure at 50 °C with 40 %RH is 92.51(torr) \times 40(%) = 37.0(torr) which yields 32.7 °C as dew point in case of 50 °C and 40 %RH. Therefore, the error in dew point between theoretical and experimental data is as small as 32.6 - 32.7 = -0.1 °C.

Table 1. The specification of KARI's thermal humidity chamber system

Description	Specification	
Working Volume	3.6(W)×3.8(L)×5.0(H) (m)	0.8(W)×0.8(L)×0.8(H) (m)
External Dimensions	4.0(W)×6.2(L)×6.5(H) (m)	1.6(W)×1.8(L)×1.9(H) (m)
Overall Temperature Range	-150 °C to +120 °C	-150 °C to +150 °C
Thermal Control Mode	(1) LN2 Cooling Mode: Min. temp : -150 °C (Within 60 min. from +120 °C to -150 °C) (2) Mechanical Cooling Mode : Min. temp : - 70 °C (Within 100 min. from +120 °C to -70 °C) (3) Heating Mode : Max. temp : +120 °C (Within 50 min. from -150 °C to +120 °C)	(1) LN2 Cooling Mode: Min. temp : -150 °C (Within 30 min. from +150 °C to -150 °C) (2) Mechanical Cooling Mode : Min. temp : - 70 °C (Within 90 min. from +150 °C to -70 °C) (3) Heating Mode : Max. temp : +150 °C (Within 60 min. from -150 °C to +150 °C)
Humidity Control Mode	20 < RH <95 % (in the range of 5 to 85 °C)	20 < RH <95 % (in the range of 5 to 85 °C)
Control Stability (at soak period)	Temperature : ±1 °C Humidity : ±3 %RH	Temperature : ±1 °C Humidity : ±3 %RH
GN2 Purging	RH <5 % at room temperature	RH <5 % at room temperature
Other features	2 platforms to introduce a satellite into the chamber Door type : 2 hinged door	Door type : 1 hinged door



(a) P vs. T



(b) log(P) vs. (T+C)-1 for linear correlation

Fig. 1. Saturated vapor pressure of water at various temperature

Eq. (4) can also be used to make a prediction about the change of relative humidity(RH₁ → RH₂) according to temperature variation(T₁ → T₂) in case of no net change of the amount of water vapor in a confined system of interest where dew point is invariable. From the fact that T_{dew}(T₁, RH₁) = T_{dew}(T₂, RH₂) in Eq. (4), the following relation is deduced to estimate a new relative humidity level according to variation of temperature.

$$\log(RH_2) - \frac{B}{T_2 + C} = \log(RH_1) - \frac{B}{T_1 + C}$$

$$\therefore RH_2 = RH_1 \times 10^{\left(-\frac{B}{T_2 + C} + \frac{B}{T_1 + C}\right)} \quad (5)$$

Prediction of mass of water vapor

Thermal humidity simulator requires an adequate supply of liquid water from water source like filtered tap water or de-ionized water to simulate a wide range of humidity level. Therefore, prediction of mass of water vapor makes it possible to make a rough estimation for the necessary minimum amount of supplied liquid water and the water boiler capacity during humidity simulation. Mass of water vapor occupying a volume of a cubic meter(m^3) at temperature T ($^{\circ}C$) with relative humidity RH (%RH) is predicted in two methods as follows :

Method 1

- 1) Obtain the mass of saturated water vapor at temperature T ($^{\circ}C$) from Table 5.27 in Lange's handbook[2].
- 2) Multiply the mass of saturated water vapor obtained from 1) by the relative humidity, RH/100, to get the mass of water vapor.

Method 1 requires somewhat cumbersome work of referring to the table 5.27 in the process of seeking the mass of saturated water vapor. For more efficient and systematic solution, therefore, it is necessary to find out more organized approach like method 2 as below.

Method 2

- 1) Estimate the partial pressure of water vapor(P_w) from Eq. (3).
- 2) Use the ideal-gas equation of state to estimate the density of water vapor ρ_w (g/m^3) at temperature T ($^{\circ}C$) as follows :

$$\rho_w = \frac{P_w}{R_w(T + 273.15)} = \frac{P_w}{(R_u/M_w)(T + 273.15)} \quad (6)$$

Therefore, from Eqs. (3) and (6), the mass of water vapor(Mass_w) in a volume of a cubic meter at temperature T ($^{\circ}C$) with relative humidity RH (%RH) is

$$Mass_w = \rho_w = \frac{10^{\left(A - \frac{B}{T + C}\right)} \times RH/100}{(R_u/M_w)(T + 273.15)} (g/m^3) \quad (7)$$

Analysis of dehumidification process by GN2 purge mode

Dehumidification process plays a crucial role in performing thermal cycling test and storage process of satellites. During the period of KOMPSAT-1 PFM storage, for example, a relative humidity of less than 30 % with a goal to keep the storage below 15 % is recommended to minimize any moisture related aging problems.[3] Maintaining a relative humidity below 15 % in the thermal humidity chamber requires some pertinent dehumidification processes either by refrigeration coils that remains just above water freezing point($0^{\circ}C$) or by purge process of gaseous nitrogen(GN2) that is supplied from nitrogen storage tanks located outside the test area. In this section, dehumidification process by GN2 purge will be theoretically evaluated by proposing a simplified GN2 purge model to anticipate the degree of decrease of a relative humidity in the large-sized thermal humidity chamber. The schematic of GN2 purge process in the thermal humidity chamber is delineated in Fig. 2. It is noted in Fig. 2 that all the gas which is supplied through inlet ports at the rear of the chamber is only nitrogen while the exhausted gas through the outlet port at the top of the chamber is a mixture of nitrogen and moisture-containing air which originally occupies the inner space of the chamber prior to GN2 purge. Now a simple GN2

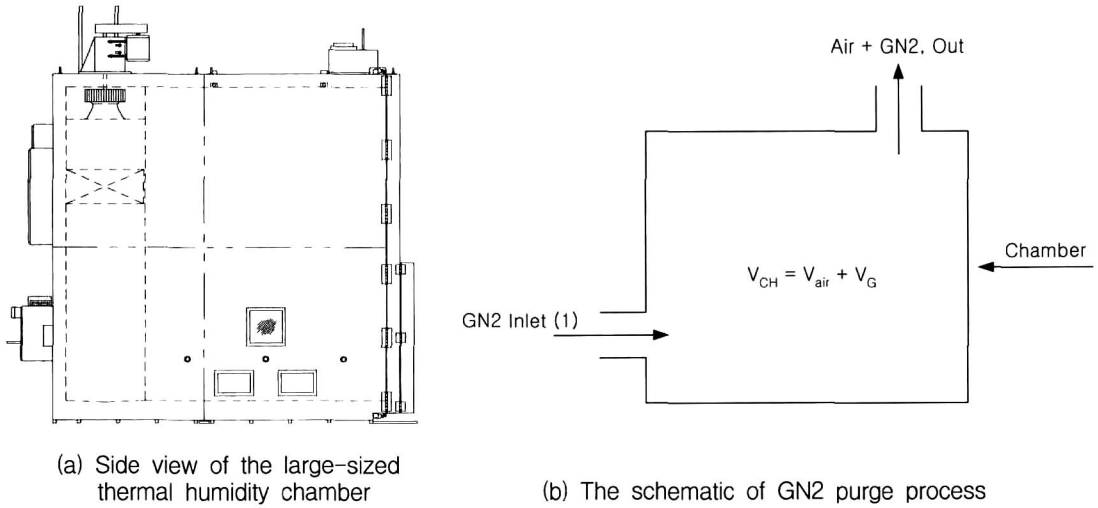


Fig. 2. The schematic of GN2 purge process in the large-sized thermal humidity chamber

purge model can be established by assuming that the flow rate of each exhaust gas is proportional to the volumetric amount of the gas remaining in the chamber, namely,

$$\frac{d V_{air}}{dt} = a V_{air} , \quad \frac{d V_{G,out}}{dt} = b V_G \quad (a, b : \text{negative constant}) \quad (8)$$

Eq. (8) can be combined into one equation as following.

$$\frac{d V_{G,out}/dt}{d V_{air}/dt} = k \frac{V_G}{V_{air}} \quad (9)$$

where k is characteristic purge constant of a chamber.

The fact that GN2 and air are all the gases that occupy the volume of the chamber interior leads to the following.

$$V_G + V_{air} = V_{CH} \quad (10)$$

A constant pressure in the chamber during GN2 purge process allows the conservation of the volumetric flow rate between GN2 inlet port and the exhaust port as below.

$$I + \frac{d V_{G,out}}{dt} + \frac{d V_{air}}{dt} = 0 \quad (11)$$

Elimination of $\frac{d V_{G,out}}{dt}$ from Eqs. (9) and (11) and substitution of V_G with $(V_{CH} - V_{air})$ from Eq. (10) yield the function of only V_{air} as follows.

$$\frac{d V_{air}(t)}{dt} \left(1 - k + \frac{V_{CH}}{V_{air}(t)} \right) + I = 0 \quad (12)$$

Multiplying dt on both sides of Eq. (12) and integrating with the initial condition that $V_{air} = V_{CH}$ at $t = 0$ yield the following.

$$I \times t = (1 - k)(V_{CH} - V_{air}(t)) - V_{CH} \times \ln\left(\frac{V_{air}(t)}{V_{CH}}\right) \quad (13)$$

At this point, a reasonable assumption that relative humidity is proportional to the volume of air in the chamber (V_{air}) can be made from the consideration that a constant ratio of the amount

of moisture to that of air is presupposed inside the chamber because moisture and air together constitute a form of wet air and, therefore, moisture and air are not considered to be separable. This assumption is described in a simple form as following.

$$\frac{RH(t)}{RH_i} = \frac{V_{air}(t)}{V_{CH}} \quad (14)$$

Where RH_i is an initial value of relative humidity in the chamber.

Combination of Eqs. (13) and (14) yields the function of relative humidity with respect to time as below.

$$-\frac{I}{V_{CH}} t = (1 - k)(1 - \frac{RH(t)}{RH_i}) - \ln(\frac{RH(t)}{RH_i}) \quad (15)$$

V_{CH} is $3.6(W) \times 3.8(D) \times 5.0(W) = 68.4(m^3)$. GN2 inlet flow rate, I , is measured from GN2 flow meter located at GN2 inlet port of the chamber. Eq. (15) makes it possible to make a theoretical prediction of the decrease of relative humidity(RH) with respect to time(t) during GN2 purge process.

Thermal Humidity Chamber System

Various thermal humidity tests were performed to verify the theoretical prediction of humidity characteristics by using two thermal humidity chambers, one of which is a large-sized thermal humidity chamber used for the storage and thermal-humidity cycling tests of the KOMPSAT-1 PFM(Korea Multi Purpose Satellite-1 Proto Flight Model)[4,5] and the other one is a small-sized thermal humidity chamber used for the thermal-humidity cycle tests of a variety of components whose function needs to be verified under specified thermal and humid conditions.

Fig. 3 shows the overall view of a large-sized thermal humidity chamber with KOMPSAT-1 PFM satellite being



Fig. 3. The overall view of a large-sized thermal humidity chamber and KOMPSAT-1 PFM located in front of the chamber

introduced into the chamber interior just prior to the thermal cycling test of KOMPSAT-1 PFM in July 2000. Major specification of a large-sized thermal humidity chamber is summarized in Table 1. Fig. 4 shows the overall view of a small-sized thermal humidity chamber whose major specification is also in Table 1. The small-sized thermal humidity chamber vessel is a rectangular type with a hinge-type door. Test modes of these thermal humidity chamber system consist of not only thermal control mode such as LN2 cooling, mechanical cooling, and heating mode but also humidity control mode such as humidification/dehumidification including GN2 purge mode. LN2 cooling mode applies direct injection method through spiral nozzles to simulate $-150\text{ }^{\circ}\text{C}$. Mechanical cooling mode utilizes conventional cascade-type refrigeration system. Humidity mode is achieved by wet heating system that consists of wet heater elements, a small pump for water supply, a water boiler container, a filter, and de-ionizer. Dehumidification is accomplished by activating the refrigeration unit dedicated to dehumidification. The temperature conditioning area located at the rear part of the chamber interior includes evaporators of refrigeration system, LN2 injection spiral nozzles, STS pipe sheaths heater elements, and wet heater elements. Two circulation fans are designed and installed above the temperature conditioning areas to promote

effective air circulation and enhance temperature uniformity in the chamber. The exhaust damper is located at the top of the chamber to exhaust excessive gas. Ever since the installation of the chamber system had been completed, various tests have been performed for each mode. This paper, however, focuses on humidity control mode to provide experimental humidity data for verification of theoretical analysis of humidity characteristics.

Results and Discussion

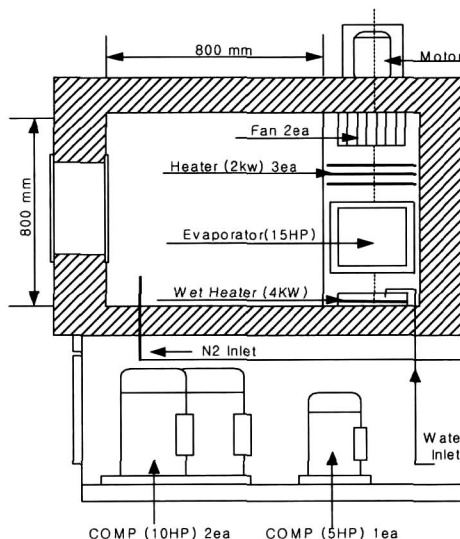
In Fig. 5, theoretical estimation for relative humidity according to temperature variation was compared and verified with experimental data. In Fig. 5, with the initial air temperature of 70 °C and humidity of 8.5 %RH in the confined volume of a large-sized humidity chamber, the air cooled down slowly to the ambient which resulted in slow increase of relative humidity. Fig. 5 shows that the humidity level estimated theoretically using Eq. (5) is considered to be in fairly good agreement with experimental humidity data because the maximum difference between theoretical and experimental data is only 2 %RH, which is just within the measurement error of humidity sensor itself.

Fig. 6 shows the amount of water vapor necessary to simulate various thermal humid conditions in a unit volume of a confined space. Fig. 6(a) indicates that the necessary amount of water vapor increases exponentially with increasing temperature at constant humidity. For example, as for the relative humidity of 50 %, the amount of water is 8.7 g per cubic meter(m³) at 20 °C and 15.2 g at 30 °C, whose difference yields 6.5 g / 10 °C = 0.65 g/°C in the range of 20 ~ 30 °C while, for the case of hot temperature, the amount of water is 98.2 g at 70 °C and 145.0 g at 80 °C, whose difference yields 46.8 g / 10 °C = 4.68 g/°C in the range of 70 ~ 80 °C, which is more than seven times as much as the amount in the range of 20 ~ 30 °C. Namely, the amount of water vapor necessary to maintain constant humidity increases exponentially with increasing temperature. On the other hand, at constant temperature, the amount of water vapor is just proportional to the humidity level as shown in Fig. 6(b).

Fig. 7 delineates the theoretical estimation, which is evaluated by Eq. (15), of the trend of relative humidity and makes comparison with experimental data during GN₂ purge process.



(a) Front view with a door open



(b) Schematic of left side view

Fig. 4. A small-sized thermal humidity chamber

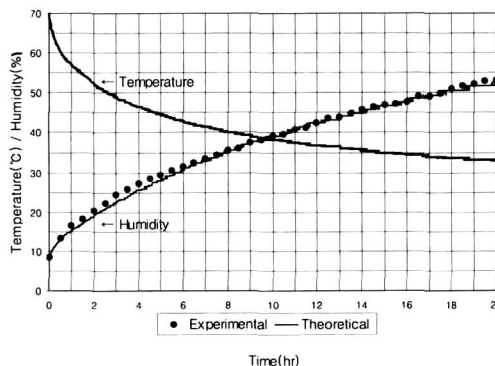
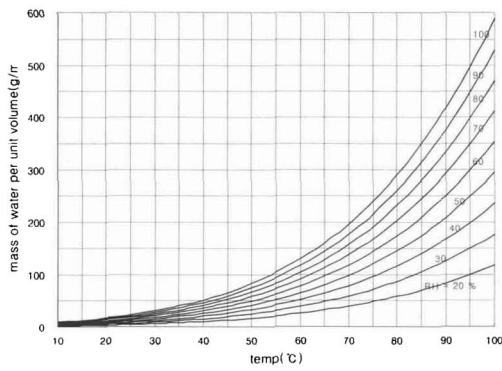
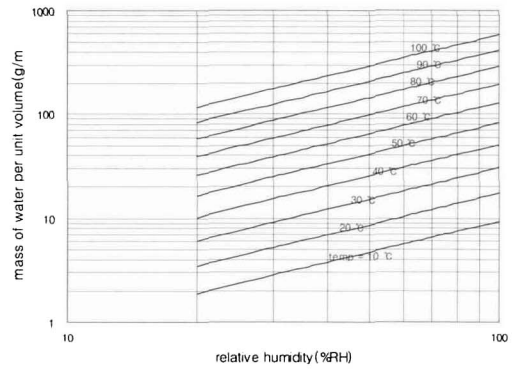


Fig. 5. Trend of variation of relative humidity according to temperature variation



(a) mass of water vs. temperature



(b) mass of water vs. relative humidity

Fig. 6 Mass of water vapor at various temperature and humidity level

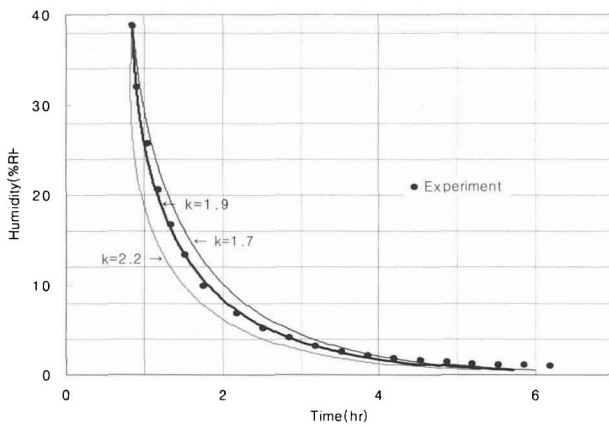


Fig. 7. Theoretical estimation for the trend of relative humidity level during GN2 purge process and comparison with experimental data (GN2 input = 30 scfm)

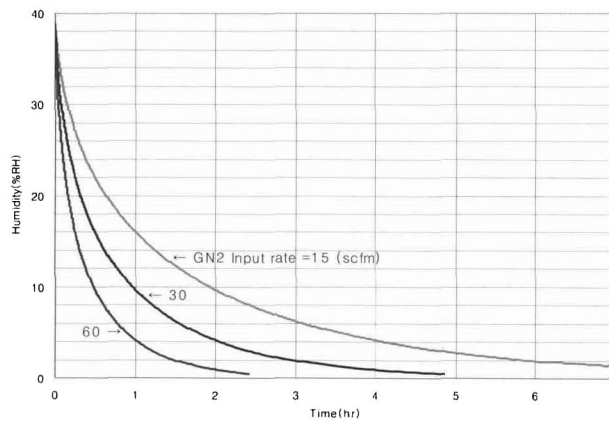


Fig. 8. Theoretical estimation of the trend of relative humidity level for various GN2 input during GN2 purge process (k=1.9)

Fig. 7 shows that theoretical trend is in good agreement with experimental data for $k=1.9$, which is, subsequently, most suitable for characteristic purge constant of the large-sized humidity chamber. Of course, characteristic purge constant may be different for the small-sized humidity chamber because this constant is considered to depend on chamber configuration and GN2 purge mechanism which may be different from chamber to chamber. Experimental data in Fig. 7 is obtained from GN2 inlet flow rate, I , of 30 scfm. Therefore, V_{CH}/I in Eq. (15) is estimated from Eq. (16) as below.

$$\frac{V_{CH}}{I} = \frac{68.4(m^3)}{30(ft^3/min)} = \frac{68.4}{(30 \times 0.33 \times 60)} = 1.4(hr) \quad (16)$$

Fig. 8 shows the trends of relative humidity which is theoretically estimated with $k=1.9$ for various GN2 inlet flow rate. In case of GN2 flow rate of 60 scfm, it takes 0.16 hours for humidity to reduce from 40 % to 20 %, and 0.48 hours to reduce from 40 % to 10 %, and 0.89 hours to reduce from 40 % to 5 %. In case of GN2 flow rate of 30 scfm, it takes 0.32, 0.97, 1.77 hours to reduce from 40 % to 20, 10, 5 %, respectively. It means that, if GN2 flow rate

reduces by half, for example 60 to 30 scfm as in the above case, the efficiency of GN2 purge reduces by half and, consequently, it takes twice as long to reach a certain humidity level as in case of 60 scfm. Similarly, in case of GN2 flow rate of 15 scfm, which is half of 30 scfm, the efficiency of GN2 purge reduces by half and it takes twice as long to reach a certain humidity level as in case of 30 scfm. Generally speaking, time elapsed to reach a certain humidity level, t , is reversely proportional to GN2 inlet flow rate, I , as is also explained by the fact that $I \times t$ is constant for a fixed RH(t) in Eq. (15).

Conclusions

Theoretical prediction of relative humidity according to temperature variation was made based on a saturated vapor pressure-temperature curve of water. This prediction showed good agreement with experimental data obtained from various test results of two thermal humidity chambers.

The characteristics of dew point showed that the higher the temperature or the humidity is, the higher the dew point is. However, the higher the humidity is, the less susceptible the dew point is to the humidity variation while the susceptibility of dew point to temperature variation is almost constant regardless of temperature range.

From the estimation of the amount of water vapor necessary to simulate various thermal humid conditions in a unit volume of system, the amount of water vapor necessary to maintain constant humidity was found to increase exponentially with increasing temperature while the amount of water vapor is just proportional to the humidity level at constant temperature.

A simple but well-fitting model of dehumidification process provided quite reasonable prediction, compared with experimental data, about the trend of relative humidity level during GN2 purge process in a humidity chamber. Characteristic purge constant was found to be $k=1.9$ of the large-sized humidity chamber. It takes about 1 hour to reduce from 40 %RH to 20 %RH with GN2 flow rate of 30 scfm. The lower the GN2 inlet flow rate is, the longer the time is taken to reach a certain humidity level in such manner that the elapsed time is reversely proportional to GN2 inlet flow rate.

Further experimental and theoretical researches are encouraged for more thorough understanding and useful information about thermal-humidity characteristics.

Acknowledgement

Authors wish to acknowledge that this work was supported by Advanced Backbone IT Technology Development Project of Ministry of Information and Communication (Code ID. IMT2000-A1-2).

References

1. S.W. Choi, J.H. Cho, J.M. Choi, "Thermal Environmental Test for Koreanized Component of KOMPSAT," Proceedings of the KSAS Fall Annual Meeting, Seoul, Korea, Nov. 1997
2. John, A. D., "Lange's Handbook of Chemistry," 14th ed., McGraw Hill, 1992
3. Kiran, J., "KOMPSAT Proto-flight Model Storage Plan," CDRL No. SE-19, TRW, CA, 28 Feb. 1997
4. J.H. Cho, S.W. Choi, H.J. Seo, S.S. Lee, "Thermal Cycle Test for KOMPSAT-1 PFM," Proceedings of the KSAS Fall Annual Meeting, Ulsan, Korea, Nov. 2000
5. J.H. Cho, S.W. Choi, H.J. Seo, S.S. Lee, "Performance Test of Thermal/Humidity Cycling Chamber for Satellite Storage and Test," Proceedings of the KSAS Fall Annual Meeting, Ulsan, Korea. Nov. 2000